

# Orthogonal non-Gaussianity in DBI Galileon: constraints from WMAP9 and prospects for Planck

Kazuya Koyama<sup>1</sup>, Guido Walter Pettinari<sup>1</sup>, Shuntaro Mizuno<sup>2,3</sup>, Christian Fidler<sup>1</sup>

<sup>1</sup> *Institute of Cosmology & Gravitation, University of Portsmouth,  
Dennis Sciama Building, Portsmouth, PO1 3FX, United Kingdom*

<sup>2</sup> *APC (CNRS-Université Paris 7), 10 rue Alice Domon et Léonie Duquet,  
75205 Paris Cedex 13, France*

<sup>3</sup> *Laboratoire de Physique Théorique, Université Paris-Sud 11 et CNRS,  
Bâtiment 210, 91405 Orsay Cedex, France*

## Abstract

In this note, we study constraints on primordial non-Gaussianity in DBI Galileon models in which an induced gravity term is added to the Dirac-Born-Infeld (DBI) action. In this model, the non-Gaussianity of orthogonal shape can be generated, which is slightly favoured by WMAP nine-year (WMAP9) data. We provide a relation between theoretical parameters and orthogonal/equilateral non-linear parameters using the Fisher matrix approach. In doing so, we include the effect of the CMB transfer functions and Planck noise properties by employing the recently developed **SONG** code. The relation is also shown in the effective theory language so that it can be applied to general single-field models. Using the bispectrum Fisher matrix for Planck, we derive forecasts for constraints on the theoretical parameters. We find that Planck can rule out the conventional DBI inflation model at a statistically significant level, provided that it measures the same central values as WMAP9 for equilateral and orthogonal non-Gaussianities.

## 1 Introduction

Primordial non-Gaussianity of the curvature perturbation provides valuable information on the physics in the very early Universe [1]. Non-linearity of quantum fluctuations during inflation gives rise to a bispectrum in the Cosmic Microwave Background (CMB) temperature anisotropies that peaks for equal-side triangles [2]. The most popular model for the equilateral type non-Gaussianity is the Dirac-Born-Infeld (DBI) inflation model [3]. In the DBI inflation model, the inflaton is identified as the position of a D3-brane in a higher dimensional spacetime. The DBI action that describes the motion of the brane is a non-linear function of the kinetic term of the inflaton, which leads to the non-Gaussianity of quantum fluctuations. While the original DBI inflation model considered only the motion and fluctuations in the radial direction, we can consistently take into account the dynamics and fluctuations in the angular directions [4] (see also [5, 6]). Although the original single field DBI inflation model [3] is under strain from an additional requirement related with the compactification scheme of the string theory [7, 8], this can be evaded in multi-field DBI inflation models and the shape of the bispectrum remains as in the single-field model [4].

Recently, a natural extension of the DBI inflation model has been obtained by adding an induced gravity term [10, 11]. This leads to the quartic Galileon Lagrangian [12] when the motion of the brane

is non-relativistic. Thus this model is dubbed as the DBI Galileon model [13]. This is one of a very few models where the non-Gaussianity of orthogonal shape can be generated [10]. The orthogonal shape of non-Gaussianity was originally discovered in the context of the effective theory of inflation [14], which has a minimum overlap between local and equilateral non-Gaussianities [15]. In the WMAP nine-year (WMAP9) data, a hint was found that the orthogonal type non-Gaussianity could be non-zero at  $2\sigma$  level when the equilateral non-Gaussianity is included in the parameter space [9]. This result is far from conclusive and it needs to be confirmed by the Planck satellite.

In this note, we provide a relation between the equilateral and orthogonal templates, parametrised respectively by the non-linear parameters  $f_{\text{NL}}^{\text{eq}}$  and  $f_{\text{NL}}^{\text{orth}}$ , and the theoretical parameters in the DBI Galileon models by properly taking into account the CMB transfer functions and Planck noise properties. We also derive the constraints on  $f_{\text{NL}}^{\text{eq}}, f_{\text{NL}}^{\text{orth}}$  expected from Planck, including the possibility of the simultaneous presence of the two shapes in the data. We then provide forecasts for the constraints on the parameters in the DBI Galileon model. We also present these constraints in the effective theory language so that they can be easily applied to more general single-field models.

This paper is organised as follows. In section 2, we summarise the prediction of non-Gaussianity in the DBI Galileon models. In section 3, we present the equilateral and orthogonal templates and discuss the overlap between theoretical bispectrum shapes and these templates. In section 4, we apply the WMAP9 results to obtain constraints on the theoretical parameters. We study forecasts for Planck in section 5. We compute the bispectrum Fisher matrix for Planck and use it to provide a relation between observational templates and theoretical parameters. Similarly, we provide Planck forecasts for the two parameters in the DBI Galileon model and those in the effective theory. Section 6 is devoted to the conclusion.

## 2 Non-Gaussianity in DBI Galileon model

In this section, we summarise the set-up of the DBI Galileon model and its predictions for the non-Gaussianity by following Refs. [10, 11]. We consider a D3-brane with tension  $T_3$  evolving in a 10-dimensional geometry described by the metric

$$ds^2 = h^{-1/2}(y^K) g_{\mu\nu} dx^\mu dx^\nu + h^{1/2}(y^K) G_{IJ}(y^K) dy^I dy^J \equiv H_{AB} dY^A dY^B, \quad (1)$$

with coordinates  $Y^A = \{x^\mu, y^I\}$ , where  $\mu = 0, \dots, 3$  and  $I = 1, \dots, 6$ . The induced metric on the 3-brane is given by

$$\gamma_{\mu\nu} = H_{AB} \partial_\mu Y_{(b)}^A \partial_\nu Y_{(b)}^B, \quad (2)$$

where the brane embedding is defined by the functions  $Y_{(b)}^A(x^\mu)$ , with  $x^\mu$  being the spacetime coordinates on the brane. We choose the brane embedding as  $Y_{(b)}^A = (x^\mu, \varphi^I(x^\mu))$ . Then the induced metric can be written as

$$\gamma_{\mu\nu} = h^{-1/2} (g_{\mu\nu} + h G_{IJ} \partial_\mu \varphi^I \partial_\nu \varphi^J). \quad (3)$$

The action in the DBI Galileon model is given by

$$S = \int d^4x \left[ \frac{M_P^2}{2} \sqrt{-g} R[g] + \frac{M^2}{2} \sqrt{-\gamma} R[\gamma] + \sqrt{-g} \mathcal{L}_{\text{brane}} \right], \quad (4)$$

where  $M_P$  and  $M$  are constant mass scales and

$$\mathcal{L}_{\text{brane}} = -\frac{1}{f(\phi^I)} (\sqrt{\mathcal{D}} - 1) - V(\phi^I). \quad (5)$$

The second term in the action is the induced gravity term, which is absent in the conventional DBI inflation model. Here, we have introduced the rescaled variables using the tension of the D3 brane,  $T_3$ ,

$$f = \frac{h}{T_3}, \quad \phi^I = \sqrt{T_3} \varphi^I, \quad (6)$$

we included potential terms in the brane action and we defined

$$\mathcal{D} \equiv \det(\delta_\nu^\mu + f G_{IJ} g^{\mu\rho} \partial_\rho \phi^I \partial_\nu \phi^J), \quad (7)$$

where  $G_{IJ}(\phi^K)$  will play the role of a metric in the space of the scalar fields  $\phi^I$ . By defining the mixed kinetic terms for the scalar fields

$$X^{IJ} \equiv -\frac{1}{2} g^{\mu\nu} \partial_\mu \phi^I \partial_\nu \phi^J, \quad (8)$$

it has been shown that the explicit expression of  $\mathcal{D}$  reads [4]

$$\mathcal{D} = 1 - 2f G_{IJ} X^{IJ} + 4f^2 X_I^{[I} X_J^{J]} - 8f^3 X_I^{[I} X_J^J X_K^{K]} + 16f^4 X_I^{[I} X_J^J X_K^K X_L^{L]}, \quad (9)$$

where the brackets denote antisymmetrisation on the field indices and  $X_I^J = G_{IK} X^{KJ}$ . Similarly, one can express  $\sqrt{-\gamma} R[\gamma]$  in terms of the fields and the geometrical quantities associated to the cosmological metric, leading to a multifield relativistic extension of the quartic Galileon Lagrangian in curved spacetime.

In this paper, for simplicity, we only consider the single-field model where we can ignore the dynamics of angular directions and the late time curvature perturbation is dominated by the radial fluctuations. There are two parameters in the single field model. One is the background value of  $\mathcal{D}$ :

$$c_D^2 \equiv 1 - f \dot{\sigma}^2, \quad (10)$$

where  $\dot{\sigma} \equiv \sqrt{G_{IJ} \dot{\phi}^I \dot{\phi}^J}$  plays the role of an effective collective velocity of the fields. In the DBI inflation model,  $c_D$  corresponds to the sound speed of the perturbations,  $c_s$ . The other parameter characterises the effect of the induced gravity

$$\alpha \equiv \frac{f H^2 M^2}{c_D^2 \sqrt{h}}, \quad (11)$$

where  $H$  is the Hubble parameter. If  $\alpha = 0$  we reproduce the DBI inflation model. The parameter  $\alpha$  is restricted to be  $0 \leq \alpha \leq 1/9$ .

We only show the final results for the non-Gaussianity of the gravitational potential. Detailed calculations can be found in Refs. [10, 11]. The bispectrum of the Newtonian potential  $\Phi$  has the form

$$\langle \Phi_{\vec{k}_1} \Phi_{\vec{k}_2} \Phi_{\vec{k}_3} \rangle = (2\pi)^3 \delta^{(3)}(\vec{k}_1 + \vec{k}_2 + \vec{k}_3) S(k_1, k_2, k_3), \quad (12)$$

where  $S$  is the primordial bispectrum shape and the Dirac delta enforces spatial homogeneity. In the single-field DBI Galileon model, two bispectrum shapes arise [15]:

$$\begin{aligned} S^{(\text{grad})}(k_1, k_2, k_3) &= -\frac{27}{17} f_{\text{NL}}^{\text{grad}} \Delta_\Phi^2 \\ &\times \frac{(24K_3^6 - 8K_2^2 K_3^3 K_1 - 8K_2^4 K_1^2 + 22K_3^3 K_1^3 - 6K_2^2 K_1^4 + 2K_1^6)}{K_3^9 K_1^3}, \\ S^{(\text{time})}(k_1, k_2, k_3) &= 162 f_{\text{NL}}^{\text{time}} \Delta_\Phi^2 \cdot \frac{1}{K_3^3 K_1^3}. \end{aligned} \quad (13)$$

where

$$\begin{aligned} K_1 &= k_1 + k_2 + k_3, \\ K_2 &= (k_1 k_2 + k_2 k_3 + k_3 k_1)^{1/2}, \\ K_3 &= (k_1 k_2 k_3)^{1/3}, \end{aligned} \quad (14)$$

and we used the definition of the power spectrum

$$\langle \Phi(\vec{k}_1) \Phi(\vec{k}_2) \rangle = (2\pi)^3 \delta^{(3)}(\vec{k}_1 + \vec{k}_2) \frac{\Delta_\Phi}{k^3}. \quad (15)$$

These two shapes arise from the two distinct cubic interactions of the comoving curvature perturbation  $\zeta$ ; the first shape  $S^{(\text{grad})}$  arises from  $\dot{\zeta}(\partial_i \zeta)^2$  while the second shape  $S^{(\text{time})}$  arises from  $\dot{\zeta}^3$  [15]. The amplitudes of these bispectrum are determined by  $c_D$  and  $\alpha$  as

$$\begin{aligned} f_{\text{NL}}^{\text{grad}} &= \frac{85}{324} A^{\text{grad}} \left( 1 - \frac{1}{c_D^2} \right), & A^{\text{grad}} &= \lambda^2 \frac{1 - \alpha(9 - 2c_D^2 - 3\lambda^2)}{1 - 3\alpha(3 - 2c_D^2)}, \\ f_{\text{NL}}^{\text{time}} &= \frac{5}{81} A^{\text{time}} \left( 1 - \frac{1}{c_D^2} \right), & A^{\text{time}} &= \frac{1 - 3\alpha(5 - 2c_D^2 - 4\lambda^2 + \lambda^4)}{1 - 3\alpha(3 - 2c_D^2)}, \end{aligned} \quad (16)$$

where  $\lambda$  is the ratio between the angular and radial speed of sound

$$\lambda = \sqrt{\frac{1 - 3\alpha(3 - 2c_D^2)}{1 - \alpha(5 - 2c_D^2)}}. \quad (17)$$

### 3 CMB temperature bispectrum and templates

The shapes of the bispectrum described in section 2 are not factorisable thus it is numerically challenging to construct optimal estimators. Instead, the WMAP collaboration has been using the following equilateral [16] and orthogonal [15] templates

$$S^{(\text{eq})}(k_1, k_2, k_3) = f_{\text{NL}}^{\text{eq}} \cdot 6\Delta_{\Phi}^2 \cdot \left( -\frac{1}{k_1^3 k_2^3} - \frac{1}{k_1^3 k_3^3} - \frac{1}{k_2^3 k_3^3} - \frac{2}{k_1^2 k_2^2 k_3^2} + \frac{1}{k_1 k_2^2 k_3^3} + (5 \text{ perm.}) \right), \quad (18)$$

$$S^{(\text{orth})}(k_1, k_2, k_3) = f_{\text{NL}}^{\text{orth}} \cdot 6\Delta_{\Phi}^2 \cdot \left( -\frac{3}{k_1^3 k_2^3} - \frac{3}{k_1^3 k_3^3} - \frac{3}{k_2^3 k_3^3} - \frac{8}{k_1^2 k_2^2 k_3^2} + \frac{3}{k_1 k_2^2 k_3^3} + (5 \text{ perm.}) \right), \quad (19)$$

and gave constraints on the non-linear parameters  $(f_{\text{NL}}^{\text{eq}}, f_{\text{NL}}^{\text{orth}})$ . In order to constrain the amplitude of the galileon shapes in Eq. (13), we first need to relate  $(f_{\text{NL}}^{\text{grad}}, f_{\text{NL}}^{\text{time}})$  to the observed  $(f_{\text{NL}}^{\text{eq}}, f_{\text{NL}}^{\text{orth}})$ . To this purpose, we calculate the angular bispectrum of the CMB temperature anisotropies for all the considered shapes. The CMB bispectrum is the 3-point function of the observed temperature anisotropies

$$\langle a_{\ell_1 m_1} a_{\ell_2 m_2} a_{\ell_3 m_3} \rangle, \quad (20)$$

where  $a_{\ell m}$  are the temperature multipoles given by

$$a_{\ell m} = 4\pi(-i)^\ell \int \frac{d^3 \mathbf{k}}{(2\pi)^3} \Phi(\mathbf{k}) \Delta_\ell(k) Y_{\ell m}^*(\mathbf{k}), \quad (21)$$

and  $\Delta_\ell$  is the radiative transfer function of the temperature. By using statistical isotropy, we can define an angle-averaged bispectrum,  $b_{\ell_1 \ell_2 \ell_3}$ , as

$$\langle a_{\ell_1 m_1} a_{\ell_2 m_2} a_{\ell_3 m_3} \rangle = \begin{pmatrix} \ell_1 & \ell_2 & \ell_3 \\ m_1 & m_2 & m_3 \end{pmatrix} B_{\ell_1 \ell_2 \ell_3}. \quad (22)$$

We compute the temperature bispectrum by projecting the primordial bispectrum for the Newtonian potential in Eq. (12) on the sky today [17, 18]:

$$\begin{aligned} B_{\ell_1 \ell_2 \ell_3} &= \mathcal{G}_{0 \ 0 \ 0}^{\ell_1 \ell_2 \ell_3} \left( \frac{2}{\pi} \right)^3 \int dr r^2 \int dk_1 dk_2 dk_3 (k_1 k_2 k_3)^2 S(k_1, k_2, k_3) \\ &\quad j_{\ell_1}(rk_1) \Delta_{\ell_1}(k_1) j_{\ell_2}(rk_2) \Delta_{\ell_2}(k_2) j_{\ell_3}(rk_3) \Delta_{\ell_3}(k_3), \end{aligned} \quad (23)$$

where  $j_\ell$  is the spherical Bessel function of order  $\ell$  and  $\mathcal{G}$  are the Gaunt coefficients.

The 2D scalar product of two angular bispectra, or Fisher matrix element [17], is defined as

$$B^{(i)} \cdot B^{(j)} = \sum_{l_1 \leq l_2 \leq l_3}^{l_{\max}} \frac{B^{(i)}_{\ell_1 \ell_2 \ell_3} B^{(j)}_{\ell_1 \ell_2 \ell_3}}{\Delta_{\ell_1 \ell_2 \ell_3} C_{\ell_1} C_{\ell_2} C_{\ell_3}}, \quad (24)$$

where  $C_l$  is the angular power spectrum of temperature fluctuations,  $\Delta_{\ell_1 \ell_2 \ell_3} = 1, 2, 6$  for triangles with no, two or three equal sides, and  $l_{\max}$  is the maximum angular resolution attainable with the considered CMB survey. Note that in our analysis we include the noise contribution of the CMB survey in  $C_\ell$  as done, e. g., in Ref. [19].

Using the 2D scalar product, we obtain the relation between  $(f_{\text{NL}}^{\text{grad}}, f_{\text{NL}}^{\text{time}})$  and  $(f_{\text{NL}}^{\text{eq}}, f_{\text{NL}}^{\text{orth}})$  as [15]

$$\begin{pmatrix} f_{\text{NL}}^{\text{eq}} \\ f_{\text{NL}}^{\text{orth}} \end{pmatrix} = \begin{pmatrix} \left( \frac{B^{(\text{grad})} \cdot B^{(\text{eq})}}{B^{(\text{eq})} \cdot B^{(\text{eq})}} \right) & \left( \frac{B^{(\text{time})} \cdot B^{(\text{eq})}}{B^{(\text{eq})} \cdot B^{(\text{eq})}} \right) \\ \left( \frac{B^{(\text{grad})} \cdot B^{(\text{orth})}}{B^{(\text{orth})} \cdot B^{(\text{orth})}} \right) & \left( \frac{B^{(\text{time})} \cdot B^{(\text{orth})}}{B^{(\text{orth})} \cdot B^{(\text{orth})}} \right) \end{pmatrix}_{f_{\text{NL}}=1} \begin{pmatrix} f_{\text{NL}}^{\text{grad}} \\ f_{\text{NL}}^{\text{time}} \end{pmatrix}. \quad (25)$$

We should stress that these relations are obtained assuming that only one type of the templates is present at the same time, that is, we have either  $f_{\text{NL}}^{\text{eq}}$  or  $f_{\text{NL}}^{\text{orth}}$ . This is the same definition used by the WMAP team when they quote constraints on these non-linear parameters.

In this paper, we are interested in a joint analysis where both equilateral and orthogonal non-Gaussianity exist. For the joint analysis, we introduce a new set of non-linear parameters,  $\hat{f}^i = (\hat{f}_{\text{NL}}^{\text{eq}}, \hat{f}_{\text{NL}}^{\text{orth}})$ , which are related to  $f_i = (f_{\text{NL}}^{\text{eq}}, f_{\text{NL}}^{\text{orth}})$  as

$$\sum_j F_{ij} \hat{f}^j = F_{ii} f_i, \quad i = \text{eq, orth}, \quad (26)$$

where the template Fisher matrix  $F_{ij}$

$$F = \begin{pmatrix} B^{(\text{eq})} \cdot B^{(\text{eq})} & B^{(\text{eq})} \cdot B^{(\text{orth})} \\ B^{(\text{eq})} \cdot B^{(\text{orth})} & B^{(\text{orth})} \cdot B^{(\text{orth})} \end{pmatrix}_{f_{\text{NL}}=1} \quad (27)$$

encodes the overlap between the two observational templates in  $\ell$ -space. The new parameters,  $\hat{f}^i$ , take into account the contamination from the other type of non-Gaussianity; they are equivalent to  $f_i$  only if there is no correlation between the two estimators, that is if  $r = F_{ij}/(F_{ii}F_{jj})^{1/2} = 0$ .

Using Eqs. (25), (26) and (27), we obtain the relation between the model parameters  $(f_{\text{NL}}^{\text{grad}}, f_{\text{NL}}^{\text{time}})$  and  $(\hat{f}_{\text{NL}}^{\text{eq}}, \hat{f}_{\text{NL}}^{\text{orth}})$  as [15]

$$\begin{pmatrix} \hat{f}_{\text{NL}}^{\text{eq}} \\ \hat{f}_{\text{NL}}^{\text{orth}} \end{pmatrix} = F^{-1} M \begin{pmatrix} f_{\text{NL}}^{\text{grad}} \\ f_{\text{NL}}^{\text{time}} \end{pmatrix}, \quad M = \begin{pmatrix} B^{(\text{grad})} \cdot B^{(\text{eq})} & B^{(\text{time})} \cdot B^{(\text{eq})} \\ B^{(\text{grad})} \cdot B^{(\text{orth})} & B^{(\text{time})} \cdot B^{(\text{orth})} \end{pmatrix}_{f_{\text{NL}}=1}, \quad (28)$$

where  $M$  is the overlap matrix between the theoretical shapes and the observational templates. Given the best-fit values of  $\hat{f}^i$  from the data,  $\hat{f}_{\text{best}}^i$ , and the associated covariance matrix  $C = F^{-1}$ , we define a  $\chi^2$  statistic for model parameters  $\hat{f}^i$  as

$$\chi^2 = (\hat{f}^i - \hat{f}_{\text{best}}^i) C_{ij}^{-1} (\hat{f}^j - \hat{f}_{\text{best}}^j) = (\hat{f}^i - \hat{f}_{\text{best}}^i) F_{ij} (\hat{f}^j - \hat{f}_{\text{best}}^j). \quad (29)$$

This  $\chi^2$  statistic quantifies an agreement between the observed bispectrum and the model bispectrum.

## 4 Constraints from WMAP9

In the WMAP9 paper [9], the WMAP team gave constraints on the equilateral and orthogonal non-Gaussianity at  $1\sigma$  level as

$$f_{\text{NL}}^{\text{eq}} = 51 \pm 136, \quad f_{\text{NL}}^{\text{orth}} = -245 \pm 100. \quad (30)$$

We should again bear in mind that each of these constraints are obtained assuming the absence of the other non-Gaussianity. The template Fisher matrix obtained from the angular bispectrum is given in the WMAP9 paper as

$$F = \begin{pmatrix} B^{(\text{eq})} \cdot B^{(\text{eq})} & B^{(\text{eq})} \cdot B^{(\text{orth})} \\ B^{(\text{eq})} \cdot B^{(\text{orth})} & B^{(\text{orth})} \cdot B^{(\text{orth})} \end{pmatrix}_{f_{\text{NL}}=1} = \begin{pmatrix} 0.54 & 0.20 \\ 0.20 & 1.00 \end{pmatrix} \times 10^{-4}. \quad (31)$$

The WMAP9 paper also provided a relation between the theoretical parameters and  $(\hat{f}_{\text{NL}}^{\text{eq}}, \hat{f}_{\text{NL}}^{\text{orth}})$  in terms of the parameters of the effective field theory  $(c_s, A)$ :

$$\begin{aligned} \hat{f}_{\text{NL}}^{\text{eq}} &= \frac{1 - c_s^2}{c_s^2} (-0.276 + 0.0785A), \\ \hat{f}_{\text{NL}}^{\text{orth}} &= \frac{1 - c_s^2}{c_s^2} (0.0157 - 0.0163A). \end{aligned} \quad (32)$$

In terms of  $(c_s, A)$ , the theoretical amplitudes of the DBI Galileon shapes,  $(f_{\text{NL}}^{\text{grad}}, f_{\text{NL}}^{\text{time}})$ , are given by

$$\begin{aligned} f_{\text{NL}}^{\text{grad}} &= \frac{85}{324} \left( 1 - \frac{1}{c_s^2} \right), \\ f_{\text{NL}}^{\text{time}} &= -\frac{5}{81} A \left( 1 - \frac{1}{c_s^2} \right), \end{aligned} \quad (33)$$

which means that we can convert Eq. (32) into a relation between  $(f_{\text{NL}}^{\text{grad}}, f_{\text{NL}}^{\text{time}})$  and  $(\hat{f}_{\text{NL}}^{\text{eq}}, \hat{f}_{\text{NL}}^{\text{orth}})$  using

$$\begin{pmatrix} \hat{f}_{\text{NL}}^{\text{eq}} \\ \hat{f}_{\text{NL}}^{\text{orth}} \end{pmatrix} = \begin{pmatrix} 1.052 & 1.271 \\ -0.06 & -0.264 \end{pmatrix} \begin{pmatrix} f_{\text{NL}}^{\text{grad}} \\ f_{\text{NL}}^{\text{time}} \end{pmatrix}. \quad (34)$$

As stressed in the WMAP9 paper, the numerical values are specific to the nine-year WMAP data as they are obtained using WMAP noise properties.

We define a  $\chi^2$  statistic in terms of  $\hat{f}^i = (\hat{f}_{\text{NL}}^{\text{eq}}, \hat{f}_{\text{NL}}^{\text{orth}})$  as

$$\chi^2 = (\hat{f}^i - \hat{f}_{\text{WMAP}}^i) F_{ij} (\hat{f}^j - \hat{f}_{\text{WMAP}}^j). \quad (35)$$

The central values  $\hat{f}_{\text{WMAP}}^i$  are obtained by substituting the values of Eq. (30) into Eq. (26), and by making use of the template Fisher matrix in Eq. (34):

$$\sum_j F_{ij} \hat{f}_{\text{WMAP}}^j = F_{ii} f_{i \text{ WMAP}}, \quad f_{i \text{ WMAP}} = (51, -245). \quad (36)$$

This yields the following central values for the non-linear parameters

$$(\hat{f}_{\text{NL}}^{\text{eq}}, \hat{f}_{\text{NL}}^{\text{orth}}) = (153.1, -275.6), \quad (f_{\text{NL}}^{\text{grad}}, f_{\text{NL}}^{\text{time}}) = (-1537, 1393). \quad (37)$$

In Fig. 1, the left panel shows 68%, 95% and 99.7% confidence regions in the  $(\hat{f}_{\text{NL}}^{\text{eq}}, \hat{f}_{\text{NL}}^{\text{orth}})$  plane defined by threshold  $\chi^2$  values 2.28, 5.99 and 11.62. The right panel shows the same confidence regions in the  $(f_{\text{NL}}^{\text{grad}}, f_{\text{NL}}^{\text{time}})$  plane. We can convert these confidence regions to those of the theoretical parameters  $(c_D, \alpha)$  and  $(c_s, A)$  using Eq. (16) and Eq. (33), respectively. In Fig 2, these constraints are shown in the  $(c_s, A)$  plane in the effective theory and the  $(c_D, \alpha)$  plane in the DBI Galileon model. WMAP9 data prefers non-zero  $\alpha$  at 95% level because  $f_{\text{NL}}^{\text{orth}}$  is non-zero at 95% level. However, the DBI inflation model with  $A = -1$  or  $\alpha = 0$  is still allowed within 99.7% level.

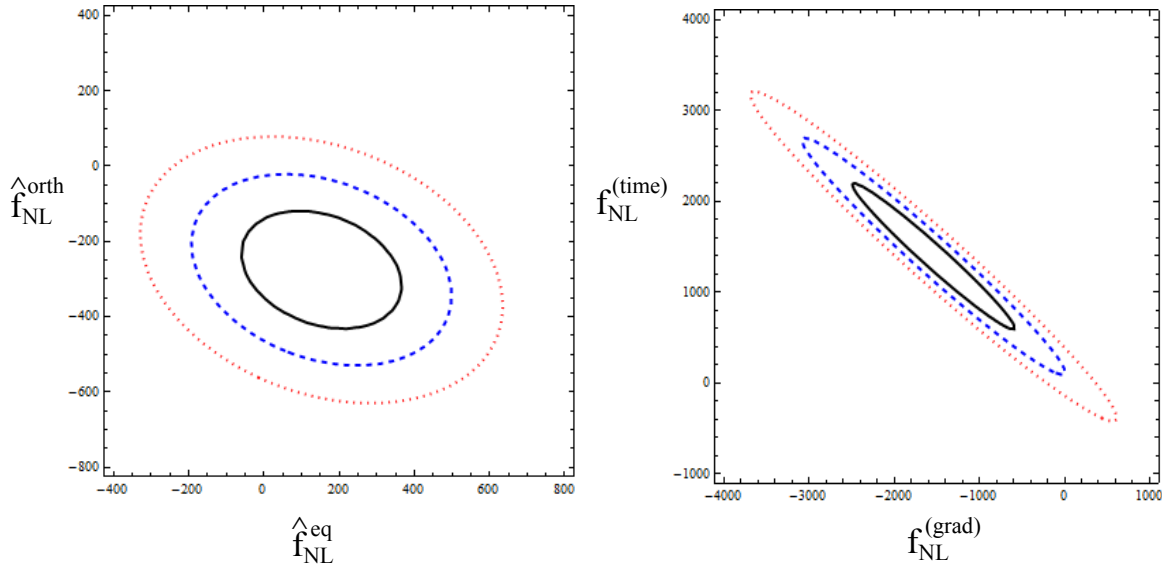


Figure 1: WMAP9 constraints on  $(f_{\text{NL}}^{\text{eq}}, f_{\text{NL}}^{\text{orth}})$  in the left panel and  $(f_{\text{NL}}^{\text{grad}}, f_{\text{NL}}^{\text{time}})$  in the right panel. 68% (black, solid), 95% (blue, dashed) and 99.7% (red, dotted) confidence contours are shown.

## 5 Constraints from Planck

In this section, we estimate how well Planck’s measurement of  $(\hat{f}_{\text{NL}}^{\text{eq}}, \hat{f}_{\text{NL}}^{\text{orth}})$  will constrain the theoretical parameters in the DBI Galileon model. We utilise the Fisher module of the Second Order Non-Gaussianity (SONG) code [20] to numerically obtain the  $F$  and  $M$  matrices which are needed to relate  $(\hat{f}_{\text{NL}}^{\text{eq}}, \hat{f}_{\text{NL}}^{\text{orth}})$  to  $(f_{\text{NL}}^{\text{grad}}, f_{\text{NL}}^{\text{time}})$  through Eq. (28). In doing so, we take into account the expected sensitivity and noise properties of Planck\*.

In order to obtain the Fisher matrices, we first estimate the bispectrum integral in Eq. (23) for the four shapes considered in this paper: equilateral, orthogonal, and the two galileon shapes in Eq. (13). The equilateral and orthogonal templates are separable in  $(k_1, k_2, k_3)$ , meaning that their computation can be conveniently split into one-dimensional integrations. The galileon shapes do not have this desirable property and we treat them as described in Sec. 5 of Ref. [20]. We obtain the temperature transfer functions  $\Delta_l(k)$  with CLASS [21] by employing a LCDM model with WMAP9 cosmological parameters [23] whereby  $h = 0.697$ ,  $\Omega_b = 0.0461$ ,  $\Omega_{\text{cdm}} = 0.236$ ,  $\Omega_{\Lambda} = 0.7181$ ,  $A_s = 2.43 \times 10^{-9}$ ,  $\tau_{\text{reio}} = 0.08$ ,  $N_{\text{eff}} = 3.04$ . Note that, since the galileon shapes were computed assuming slow-roll conditions, we consistently set  $n_s = 1$  also for the equilateral and orthogonal templates. We checked that our results do not depend on this assumption.

We compute the full  $4 \times 4$  Fisher matrix in Eq. (24) by interpolating our four numerical bispectra on a mesh in  $(\ell_1, \ell_2, \ell_3)$  [22, 20]. We employ the noise model described in Ref. [19] and consider the 100, 143, 217 GHz frequency channels of the Planck experiment, with noise and beam parameters from Ref. [24]. As a result, we obtain the following full Fisher matrix

$$F_{\text{full}} = \begin{pmatrix} 2.38 & -0.208 & 2.51 & 3.06 \\ -0.208 & 8.47 & -0.708 & -2.49 \\ 2.51 & -0.708 & 2.68 & 3.39 \\ 3.06 & -2.49 & 3.39 & 4.67 \end{pmatrix} \times 10^{-4}, \quad (38)$$

where the ordering of the rows and columns is  $f_{\text{NL}}^{\text{eq}}, f_{\text{NL}}^{\text{orth}}, f_{\text{NL}}^{\text{grad}}, f_{\text{NL}}^{\text{time}}$ . The  $F_{\text{full}}$  matrix contains all the

---

\*We plan to release the code that we used for this analysis as a separate module for the Boltzmann code CLASS [21] by the end of 2013 [22].



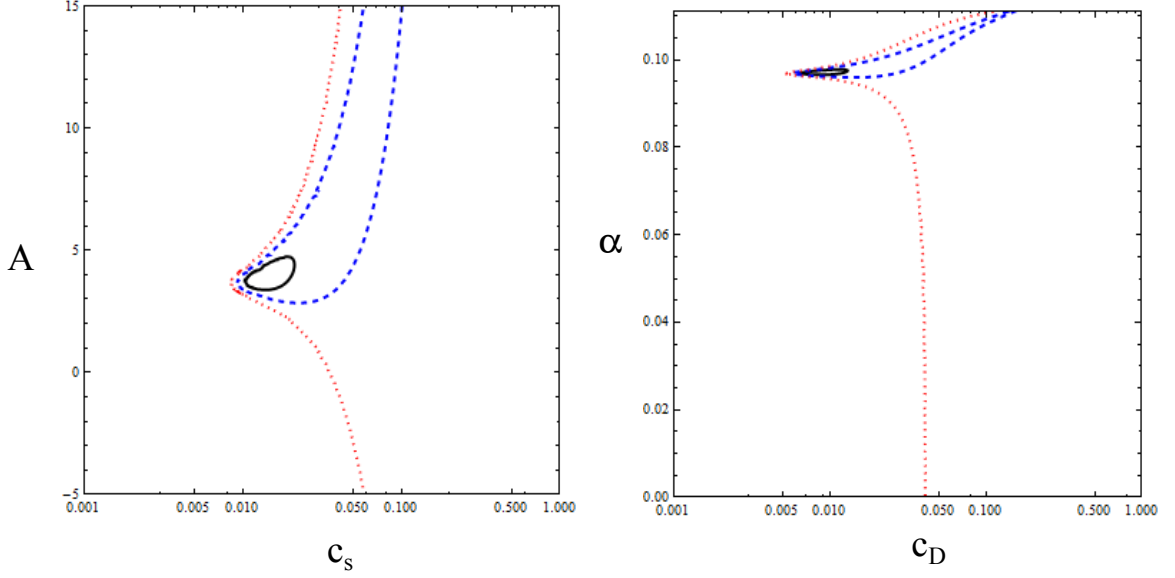


Figure 2: WMAP9 constraints on  $(c_s, A)$  in the left panel and  $(\alpha, c_D)$ . Confidence contours are the same as in Fig. 1.

information needed to produce Planck forecasts for the parameters of the DBI Galileon model. It also encodes the correlations in  $\ell$ -space between the two considered Galileon shapes (lower-right submatrix).

The  $F$  matrix is the upper-left submatrix of the full Fisher matrix

$$F = \begin{pmatrix} B^{(\text{eq})} \cdot B^{(\text{eq})} & B^{(\text{eq})} \cdot B^{(\text{orth})} \\ B^{(\text{eq})} \cdot B^{(\text{orth})} & B^{(\text{orth})} \cdot B^{(\text{orth})} \end{pmatrix}_{f_{\text{NL}}=1} = \begin{pmatrix} 2.38 & -0.208 \\ -0.208 & 8.47 \end{pmatrix} \times 10^{-4}. \quad (39)$$

The errors on  $f_{\text{NL}}^{\text{eq}}$  and  $f_{\text{NL}}^{\text{orth}}$  can be obtained as  $1/\sqrt{F_{ii}}$ , giving  $\Delta f_{\text{NL}}^{\text{eq}} = 64.8$  and  $\Delta f_{\text{NL}}^{\text{orth}} = 34.4$ . Note that these constraints do not include polarisation, which will improve the bounds by a factor of  $\mathcal{O}(2)$  [25].

The  $M$  matrix, that is the overlap between theoretical shapes and templates, is the upper-right submatrix of the full Fisher matrix in Eq. (38):

$$M = \begin{pmatrix} B^{(\text{grad})} \cdot B^{(\text{eq})} & B^{(\text{time})} \cdot B^{(\text{eq})} \\ B^{(\text{grad})} \cdot B^{(\text{orth})} & B^{(\text{time})} \cdot B^{(\text{orth})} \end{pmatrix}_{f_{\text{NL}}=1} = \begin{pmatrix} 2.51 & 3.06 \\ -0.708 & -2.49 \end{pmatrix} \times 10^{-4}. \quad (40)$$

Then the relation between  $(f_{\text{NL}}^{\text{grad}}, f_{\text{NL}}^{\text{time}})$  and  $(\hat{f}_{\text{NL}}^{\text{eq}}, \hat{f}_{\text{NL}}^{\text{orth}})$  is given by Eq. (28) as

$$\begin{pmatrix} \hat{f}_{\text{NL}}^{\text{eq}} \\ \hat{f}_{\text{NL}}^{\text{orth}} \end{pmatrix} = \begin{pmatrix} 1.048 & 1.261 \\ -0.0578 & -0.263 \end{pmatrix} \begin{pmatrix} f_{\text{NL}}^{\text{grad}} \\ f_{\text{NL}}^{\text{time}} \end{pmatrix}. \quad (41)$$

Although these numerical coefficients are specific to Planck, they are very similar to WMAP9 results. This is partly explained by the fact that the coefficients are obtained as ratios of Fisher matrix elements, i. e. they measure an overlap rather than an amplitude. We again define a  $\chi^2$  statistic

$$\chi^2 = (\hat{f}^i - \hat{f}_{\text{best}}^i) F_{ij} (\hat{f}^j - \hat{f}_{\text{best}}^j), \quad (42)$$

where  $\hat{f}_{\text{best}}^i$  are the best-fit values.

We consider two hypothetical cases. In the first scenario, we assume that Planck will measure the same central values found in WMAP9, Eq. (37) and use them as our best-fit values. In the second case, we assume



that Planck will find no evidence of non-Gaussianity ( $\hat{f}_{\text{NL}}^{\text{eq}}, \hat{f}_{\text{NL}}^{\text{orth}} = (0, 0)$ ). In Fig. 3, the left panel shows 68%, 95% and 99.7% confidence regions in the  $(\hat{f}_{\text{NL}}^{\text{eq}}, \hat{f}_{\text{NL}}^{\text{orth}})$  plane defined by threshold  $\chi^2$  values 2.28, 5.99 and 11.62. The right panel shows the same confidence regions in the  $(f_{\text{NL}}^{\text{grad}}, f_{\text{NL}}^{\text{time}})$  plane. In Fig 4, these constraints are shown in the  $(c_s, A)$  plane in the effective theory and the  $(c_D, \alpha)$  plane in the DBI Galileon model. In the first case, even at 99.7% level the contour closes in the  $(c_s, A)$  or  $(c_D, \alpha)$  planes, significantly reducing the parameter space. In particular, we can rule out the DBI inflation model ( $A = -1$  or  $\alpha = 0$ ) with high statistical significance ( $\chi^2 > 50$ ). On the other hand, in the second case, we only get a lower bound for  $c_s$  or  $c_D$ .

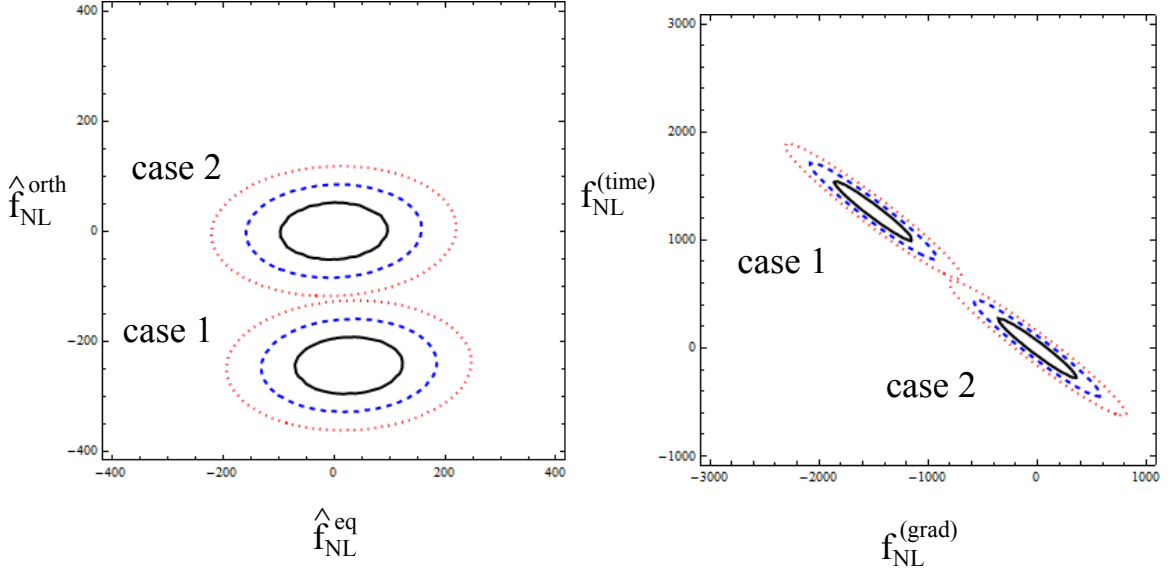


Figure 3: Planck constraints on  $(\hat{f}_{\text{NL}}^{\text{eq}}, \hat{f}_{\text{NL}}^{\text{orth}})$  in the left panel and  $(f_{\text{NL}}^{\text{grad}}, f_{\text{NL}}^{\text{time}})$  in the right panel. 68% (black, solid), 95% (blue, dashed) and 99.7% (red, dotted) confidence contours are shown.

## 6 Conclusion

In this paper, we obtained constraints on the two parameters  $(\alpha, c_D)$  in the single-field DBI Galileon model using WMAP9 results. The parameter  $\alpha$  parametrises the effect of the induced gravity on a brane and describes the deviation from the conventional DBI inflation model, while  $c_D$  becomes the sound speed in the DBI inflation limit. The WMAP9 results prefer non-zero  $\alpha$ , although the DBI inflation model is still allowed within 99.7% level. The bispectrum of the Newtonian potential in this model is not separable and it is therefore numerically challenging to construct an optimal estimator. Therefore, we used the SONG code [20] to obtain the relation between the amplitudes of theoretical bispectra  $(f_{\text{NL}}^{\text{grad}}, f_{\text{NL}}^{\text{time}})$  and the equilateral and orthogonal observational templates  $(\hat{f}_{\text{NL}}^{\text{eq}}, \hat{f}_{\text{NL}}^{\text{orth}})$  by properly taking into account the sensitivity and noise properties of Planck. We then used the bispectrum Fisher matrix for  $(\hat{f}_{\text{NL}}^{\text{eq}}, \hat{f}_{\text{NL}}^{\text{orth}})$  to predict the constraints on the two parameters.

We found that the conventional DBI inflation model would be strongly disfavoured if the Planck experiments were to confirm the central value obtained by WMAP for  $(\hat{f}_{\text{NL}}^{\text{eq}}, \hat{f}_{\text{NL}}^{\text{orth}})$ . This is driven by the non-zero “detection” of the orthogonal non-Gaussianity. At 95% level, we obtained the constraints as  $0.0964 < \alpha < 0.0973$  and  $0.007 < c_D < 0.0105$ . On the other hand, if the central values turn out to be zero, we will only obtain the lower bound for  $c_D$ . Note that our forecasts do not include polarisation, which would improve the constraints further.

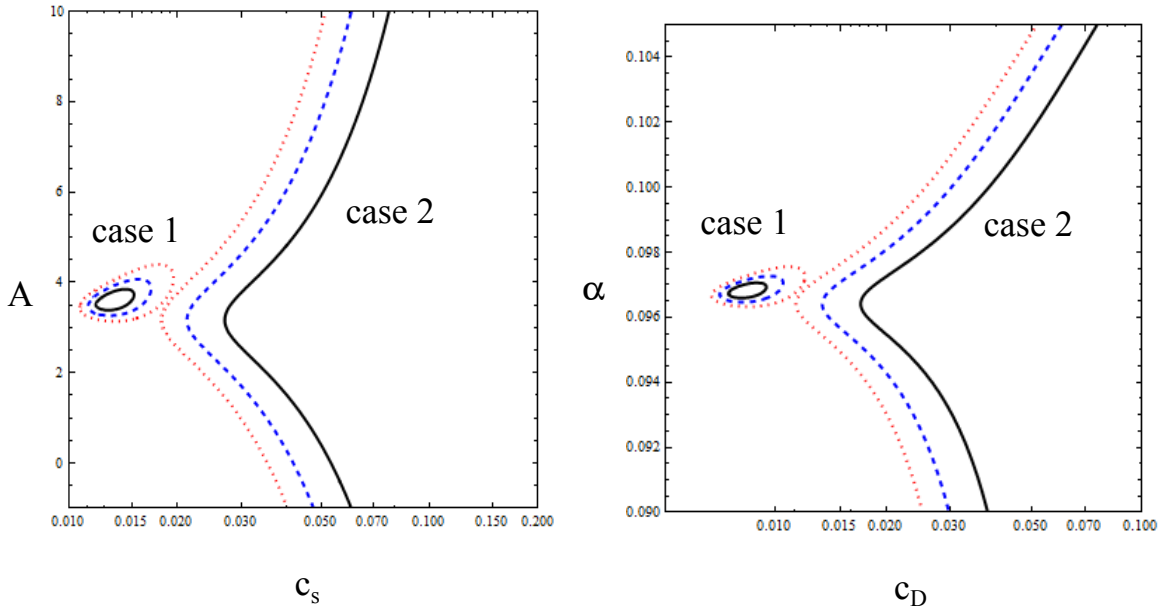


Figure 4: Planck constraints on  $(c_s, A)$  in the left panel and  $(\alpha, c_D)$  in the right panel. Confidence contours are the same as in Fig. 3.

As noticed by Ref. [26], the WMAP9 best-fit parameter for  $c_D$  tends to be small because the orthogonal shape is generated by a cancelation of the two Galileon shapes in Eq. (13). This leads to a large trispectrum as its amplitude is proportional to  $1/c_D^4$ . Thus the trispectrum will provide an additional consistency test of the model.

## Acknowledgments

We would like to thank S. Renaux-Petel for useful discussions. KK thanks G-B. Zhao for discussions on the Fisher matrix. KK and GWP are supported by the Leverhulme trust. KK and CF are supported by STFC grant ST/H002774/1. KK also acknowledges support by the European Research Council. SM is supported by CNRS.

## References

- [1] E. Komatsu, *Class. Quant. Grav.* **27**, 124010 (2010) [arXiv:1003.6097 [astro-ph.CO]].
- [2] K. Koyama, *Class. Quant. Grav.* **27**, 124001 (2010) [arXiv:1002.0600 [hep-th]].
- [3] M. Alishahiha, E. Silverstein and D. Tong, *Phys. Rev. D* **70**, 123505 (2004) [hep-th/0404084].
- [4] D. Langlois, S. Renaux-Petel, D. A. Steer and T. Tanaka, *Phys. Rev. Lett.* **101**, 061301 (2008) [arXiv:0804.3139 [hep-th]].
- [5] D. Langlois, S. Renaux-Petel, D. A. Steer and T. Tanaka, *Phys. Rev. D* **78**, 063523 (2008) [arXiv:0806.0336 [hep-th]].
- [6] F. Arroja, S. Mizuno and K. Koyama, *JCAP* **0808**, 015 (2008) [arXiv:0806.0619 [astro-ph]].
- [7] D. Baumann and L. McAllister, *Phys. Rev. D* **75** (2007) 123508 [hep-th/0610285].
- [8] J. E. Lidsey and I. Huston, *JCAP* **0707** (2007) 002 [arXiv:0705.0240 [hep-th]].
- [9] C. L. Bennett, D. Larson, J. L. Weiland, N. Jarosik, G. Hinshaw, N. Odegard, K. M. Smith and R. S. Hill *et al.*, arXiv:1212.5225 [astro-ph.CO].
- [10] S. Renaux-Petel, *Class. Quant. Grav.* **28**, 182001 (2011) [Erratum-ibid. **28**, 249601 (2011)] [arXiv:1105.6366 [astro-ph.CO]].
- [11] S. Renaux-Petel, S. Mizuno and K. Koyama, *JCAP* **1111**, 042 (2011) [arXiv:1108.0305 [astro-ph.CO]].

- [12] A. Nicolis, R. Rattazzi and E. Trincherini, Phys. Rev. D **79**, 064036 (2009) [arXiv:0811.2197 [hep-th]].
- [13] C. de Rham and A. J. Tolley, JCAP **1005**, 015 (2010) [arXiv:1003.5917 [hep-th]]; G. L. Goon, K. Hinterbichler and M. Trodden, Phys. Rev. D **83**, 085015 (2011) [arXiv:1008.4580 [hep-th]]; S. Mizuno and K. Koyama, Phys. Rev. D **82**, 103518 (2010) [arXiv:1009.0677 [hep-th]]; G. Goon, K. Hinterbichler and M. Trodden, JCAP **1107**, 017 (2011) [arXiv:1103.5745 [hep-th]].
- [14] C. Cheung, P. Creminelli, A. L. Fitzpatrick, J. Kaplan and L. Senatore, JHEP **0803**, 014 (2008) [arXiv:0709.0293 [hep-th]].
- [15] L. Senatore, K. M. Smith and M. Zaldarriaga, JCAP **1001**, 028 (2010) [arXiv:0905.3746 [astro-ph.CO]].
- [16] P. Creminelli, A. Nicolis, L. Senatore, M. Tegmark and M. Zaldarriaga, JCAP **0605**, 004 (2006) [astro-ph/0509029].
- [17] E. Komatsu and D. N. Spergel, Phys. Rev. D **63**, 063002 (2001) [astro-ph/0005036 [astro-ph]].
- [18] J. R. Fergusson and E. P. S. Shellard, Phys. Rev. D **76**, 083523 (2007) [astro-ph/0612713 [astro-ph]].
- [19] L. Pogosian, P. S. Corasaniti, C. Stephan-Otto, R. Crittenden and R. Nichol, Phys. Rev. D **72**, 103519 (2005) [arXiv:astro-ph/0506396 [astro-ph]].
- [20] G. W. Pettinari, C. Fidler, R. Crittenden, K. Koyama and D. Wands, arXiv:1302.0832 [astro-ph.CO].
- [21] D. Blas, J. Lesgourgues, and T. Tram, JCAP **034B**, 07 (2011) [arXiv:astro-ph/0506396 [astro-ph]].
- [22] G. W. Pettinari, C. Fidler, R. Crittenden, K. Koyama and D. Wands, *To be submitted in Fall 2013*.
- [23] G. Hinshaw, D. Larson, E. Komatsu, D. N. Spergel, C. L. Bennett, J. Dunkley, M. R. Nolte, M. Halpern, R. S. Hill, N. Odegard, L. Page, K. M. Smith, J. L. Weiland, B. Gold, N. Jarosik, A. Kogut, M. Limon, S. S. Meyer, G. S. Tucker, E. Wollack, E. L. Wright [arXiv:1212.5226 [astro-ph]].
- [24] K. M. Smith and M. Zaldarriaga. MNRAS, 417:219 (2011) [arXiv:astro-ph/0612571 [astro-ph]].
- [25] A. P. S. Yadav and B. D. Wandelt, Adv. Astron. **2010**, 565248 (2010) [arXiv:1006.0275 [astro-ph.CO]].
- [26] S. Renaux-Petel, arXiv:1302.6978 [astro-ph.CO].